AAS 14-304

ELASTIC MODEL TRANSITIONS: A HYBRID APPROACH UTILIZING QUADRATIC INEQUALITY CONSTRAINED LEAST SQUARES (LSQI) AND DIRECT SHAPE MAPPING (DSM)

Robert J. Jurenko,[*] T. Jason Bush,[†] and John A. Ottander[‡]

A method for transitioning linear time invariant (LTI) models in time varying simulation is proposed that utilizes both quadratically constrained least squares (LSQI) and Direct Shape Mapping (DSM) algorithms to determine physical displacements. This approach is applicable to the simulation of the elastic behavior of launch vehicles and other structures that utilize multiple LTI finite element model (FEM) derived mode sets that are propagated throughout time. The time invariant nature of the elastic data for discrete segments of the launch vehicle trajectory presents a problem of how to properly transition between models while preserving motion across the transition. In addition, energy may vary between flex models when using a truncated mode set. The LSQI-DSM algorithm can accommodate significant changes in energy between FEM models and carries elastic motion across FEM model transitions. Compared with previous approaches, the LSQI-DSM algorithm shows improvements ranging from a significant reduction to a complete removal of transients across FEM model transitions as well as maintaining elastic motion from the prior state.

INTRODUCTION

The time invariant nature of elastic data in launch vehicle simulations poses the problem of how to transition linear time invariant (LTI) finite element models (FEM) during simulation while preserving elastic motion across model transitions and ensuring there is no truncation or excitation of elastic motion. Launch vehicle controller design must consider the elastic behavior of the system as it directly impacts sensor feedback and in turn controller performance. To ensure robust controller design, Monte Carlo simulation is performed in both the frequency and time domain to evaluate effects of the elastic properties on the system. Simulation of launch vehicle elastic behavior is traditionally accomplished using discrete FEM models provided at set intervals throughout the trajectory. These models correspond to vehicle mass and other physical properties at given flight conditions along the trajectory. Dissimilarities between FEM models requires a transition methodology that captures existing elastic motion and does not introduce non-physical effects to the system.

Previous approaches to transitioning between FEM models relied on linearly interpolating the mode eigenvectors; however, there is no mathematical basis for this approach. A method for transitioning between multiple FEM models is proposed that utilizes a quadratically constrained least squares (LSQI) approach in conjunction with Direct Shape Mapping (DSM) to effect a FEM model transition that does not artificially introduce or remove energy from the system.

[*] Flight Dynamics Engineer, Leidos Inc./Jacobs ESSSA Group, Huntsville, AL 35806
[†] Engineer/Scientist, Tri-Vector Services Inc./Jacobs ESSSA Group, Huntsville, AL 35801
[‡] Engineer/Scientist, Dynamic Concepts Inc./Jacobs ESSSA Group, Huntsville, AL 35806

LSQI-DSM is based on the LSQI method,[1] which by way of an energy constraint, uses the eigenvectors of the future state $\mathbf{\Phi}_{k+1}$ and prior physical state $\mathbf{\Phi}_k$ to estimate the generalized coordinates, $\boldsymbol{\eta}$, $\dot{\boldsymbol{\eta}}$, that result in overall system energy at or below the prior state. The two key benefits of the LSQI method are that there is no requirement that the models be of similar dimension or that the eigenvectors be correlated in any way.[1]

The problem being solved is similar in nature to the topic of FEM model updating discussed in the area of structural dynamics[2,3,4,5,6] ; however, the LSQI-DSM method differs in that it is not attempting to update an existing model to experimental data, rather it looks to solve the problem of updating to an entirely new model that represents the launch vehicle structure at discrete points throughout flight. The LSQI-DSM approach presented is applicable to the simulation of the elastic behavior of launch vehicles and other structures that utilize multiple LTI FEM model derived mode sets that are propagated throughout time.

BACKGROUND

The computational burden of propagating a large number of modes in a launch vehicle simulation is significant so a subset of modes is typically selected to reduce run time. As a result of truncating or using an incomplete modal set, energy between FEM models may not be constant and could result in transients immediately following a model transition due to poorly conditioned initial states. In an effort to abate these transients, an improved methodology was developed based on the quadratic inequality least squares approach, but this new method can accommodate significant changes in energy across FEM model transitions. In the LSQI-DSM method, it is proposed that physical velocities due to elastic behavior be solved for using the previous LSQI algorithm, but solve for displacements using a two-step process that independently addresses the homogeneous (un-forced) and steady-state (forced) contributions to the elastic displacement.

Simulation results of the LSQI elastic model transition method show that while the algorithm ensures energy is not introduced across FEM model transitions, $E_{k+1} \leq E_k$, transients "ring" the system immediately following a transition, as shown in Figures 2a and 3a. While excitation is expected from physical changes to the vehicle configuration during flight such as staging and jettison events, substantial excitation due to changes in FEM models at times other than these events are non-physical artifacts of the LSQI method. An explanation was sought to determine the root cause of these transients and how to abate these effects when transitioning between FEM models. Two primary reasons were identified:

1. Running with a truncated mode set, in particular a highly truncated set, invalidates the assumption that energy is approximately constant across transitions. Figure 1 shows the effect of mode count on potential energy across multiple finite element model transitions.

2. Forcing the physical displacement ($\boldsymbol{q}_{k+1}$) and velocity ($\dot{\boldsymbol{q}}_{k+1}$) of the future state to be the final displacement ($\boldsymbol{q}_k$) and velocity ($\dot{\boldsymbol{q}}_k$) of the prior state meanwhile abruptly changing the stiffness and damping to that of the future state results in excitation as the system adjusts to instantaneous changes in stiffness and damping.

FORMULATION OF THE THEORY

Given a priori knowledge of the stiffness ($\mathbf{K}$), damping ($\mathbf{C}$), and eigenvectors ($\mathbf{\Phi}$) from the launch vehicle FEM model, the goal is to effect a smooth transition between these models and solve for the physical and generalized state at the point of FEM model transition in a manner that preserves existing elastic motion but does not truncate or excite the system in any non-physical manner. Prior to presenting the mathematical rationale for the LSQI-DSM method, background on the LSQI method is presented as it serves as a partial basis for the LSQI-DSM method.

Equations of Motion

The undamped motion is described by:

$$\mathbf{M}\ddot{\mathbf{q}} + \mathbf{K}\mathbf{q} = \mathbf{f} \tag{1}$$

where $\mathbf{M}$ is the mass matrix, $\mathbf{K}$ is the stiffness matrix, $\mathbf{f}$ is a vector of excitation forces and torques, and $\mathbf{q}$ is a vector of displacements in physical coordinates. To transform from physical to generalized coordinates the following substitutions are made to Equation (1):

$$\mathbf{q} = \mathbf{\Phi}\boldsymbol{\eta} \qquad \dot{\mathbf{q}} = \mathbf{\Phi}\dot{\boldsymbol{\eta}} \tag{2}$$

to transform the second-order equation in terms of generalized coordinates:

$$\mathbf{M}\mathbf{\Phi}\ddot{\boldsymbol{\eta}} + \mathbf{K}\mathbf{\Phi}\boldsymbol{\eta} = \mathbf{f} \tag{3}$$

Multiplying Equation (3) by the transpose of the mass-normalized eigenvector matrix ($\mathbf{\Phi}^{\mathsf{T}}$) provides:

$$\mathbf{\Phi}^{\mathsf{T}}\mathbf{M}\mathbf{\Phi}\ddot{\boldsymbol{\eta}} + \mathbf{\Phi}^{\mathsf{T}}\mathbf{K}\mathbf{\Phi}\boldsymbol{\eta} = \mathbf{\Phi}^{\mathsf{T}}\mathbf{f} \tag{4}$$

The eigenvector matrix ($\mathbf{\Phi}$) is simultaneously selected to satisfy $\mathbf{\Phi}^{\mathsf{T}}\mathbf{M}\mathbf{\Phi} = \mathbf{I}$, $\mathbf{\Phi}^{\mathsf{T}}\mathbf{K}\mathbf{\Phi} = \mathrm{diag}(\omega_n^2)$, and the orthonormality constraint. Using this selection of the eigenvector matrix allows the mass matrix term $\mathbf{\Phi}^{\mathsf{T}}\mathbf{M}\mathbf{\Phi}$ from Equation (4) to be replaced by the identity matrix ($\mathbf{I}$) and a stiffness matrix ($\widetilde{\mathbf{K}}$) where the diagonal is comprised of the natural frequencies (ω_n^2) of the elastic modes.[7]

$$\mathbf{\Phi}^{\mathsf{T}}\mathbf{M}\mathbf{\Phi} = \mathbf{I} \tag{5}$$

$$\mathbf{\Phi}^{\mathsf{T}}\mathbf{K}\mathbf{\Phi} = \widetilde{\mathbf{K}} \tag{6}$$

where

$$\widetilde{\mathbf{K}} = \begin{pmatrix} \omega_{n_1}^2 & 0 & \dots & 0 \\ 0 & \omega_{n_2}^2 & \dots & 0 \\ \vdots & \vdots & \ddots & \vdots \\ 0 & 0 & \dots & \omega_{n_m}^2 \end{pmatrix} \tag{7}$$

A constant viscous damping is typically assumed, leading to a diagonal damping matrix ($\mathbf{C}$).

$$\mathbf{C} = \begin{pmatrix} 2\zeta\omega_{n_1} & 0 & \dots & 0 \\ 0 & 2\zeta\omega_{n_2} & \dots & 0 \\ \vdots & \vdots & \ddots & \vdots \\ 0 & 0 & \dots & 2\zeta\omega_{n_m} \end{pmatrix} \tag{8}$$

On the right hand side of Equation (4) is the generalized force ($\mathbf{\Xi}$) which represents the effective loading associated with all forces and moments on the launch vehicle:

$$\mathbf{\Xi} = \mathbf{\Phi}^{\mathsf{T}}\mathbf{f} \tag{9}$$

Given the generalized coordinate transformation, an identity mass matrix, and constant viscous damping, Equation (4) can be rewritten using generalized coordinates:

$$\ddot{\boldsymbol{\eta}} + \mathbf{C}\dot{\boldsymbol{\eta}} + \widetilde{\mathbf{K}}\boldsymbol{\eta} = \mathbf{\Xi} \tag{10}$$

Energy Constraint

The least squares problem is bounded by a potential energy constraint on the generalized displacement ($\boldsymbol{\eta}$) and a kinetic energy constraint on the generalized velocity ($\dot{\boldsymbol{\eta}}$). Equation (10) is in generalized coordinates and therefore the constraints must also be formulated in generalized coordinates. Total physical displacement can be written as a sum of all modal contributions,[8] where: $\boldsymbol{\Phi}_i$ is the eigenvector and $\boldsymbol{\eta}_i$ is the generalized displacement for the i^{th} mode:

$$q = \sum_{i=1}^{\infty} \boldsymbol{\Phi}_i \boldsymbol{\eta}_i \tag{11}$$

Similarly, the total potential and kinetic energies are found by summing contributions from all modes. Using the transformations from Equation (2), an identity mass matrix (Equation (5)), and diagonal stiffness matrix (Equation (7)), the energy equations can be written in physical and generalized coordinates.

$$U = \frac{1}{2}\sum_{i}^{\infty} \mathbf{K}_{i,i}\mathbf{q}_i^2 = \frac{1}{2}\sum_{i}^{\infty} \widetilde{\mathbf{K}}_{i,i}\boldsymbol{\eta}_i^2 \tag{12}$$

$$T = \frac{1}{2}\sum_{i}^{\infty} \mathbf{M}_{i,i}\dot{\mathbf{q}}_i^2 = \frac{1}{2}\sum_{i}^{\infty} \mathbf{I}_{i,i}\dot{\boldsymbol{\eta}}_i^2 \tag{13}$$

Equations (12) and (13) represent total kinetic and potential energy assuming an infinitely large mode set. For real world applications, the maximum number of modes is finite and dictated by the FEM model. As stated earlier, computational requirements necessitate further modal reduction to a subset of the complete FEM model. For simulation purposes, the maximum number of modes, m, is a finite quantity for which the corresponding "total" potential and kinetic energies are in reality only a portion of the total physical quantities. Hereinafter, use of "total kinetic" and "total potential" will refer to the total potential (U') and kinetic (T') prescribed by the truncated mode set.

$$U' = \frac{1}{2}\sum_{i}^{m} \mathbf{K}_{i,i}\mathbf{q}_i^2 = \frac{1}{2}\sum_{i}^{m} \widetilde{\mathbf{K}}_{i,i}\boldsymbol{\eta}_i^2 \tag{14}$$

$$T' = \frac{1}{2}\sum_{i}^{m} \mathbf{M}_{i,i}\dot{\mathbf{q}}_i^2 = \frac{1}{2}\sum_{i}^{m} \mathbf{I}_{i,i}\dot{\boldsymbol{\eta}}_i^2 \tag{15}$$

Equations (14) and (15) can be written as a quadratic form. In addition, since energy is being used as a constraint to compare energy both before and after FEM model transitions, the $1/2$ multiplier can be dropped. Applying these simplifications, the energy Equations (14) and (15) reduce to:

$$U' = \boldsymbol{\eta}^{\mathsf{T}}\widetilde{\mathbf{K}}\boldsymbol{\eta} \tag{16}$$

$$T' = \dot{\boldsymbol{\eta}}^{\mathsf{T}}\dot{\boldsymbol{\eta}} \tag{17}$$

QUADRATICALLY CONSTRAINED LEAST SQUARES (LSQI) METHOD

The basis functions between FEM models are not equal ($\boldsymbol{\Phi}_\mathbf{k} \neq \boldsymbol{\Phi}_\mathbf{k+1}$), therefore a method is required to calculate the displacement ($\boldsymbol{\eta}_{k+1}$) and velocity ($\dot{\boldsymbol{\eta}}_{k+1}$) such that the elastic motion carries through the transition and there is no truncation or excitation of the system. Previously the problem was formulated as two least squares problems. To bound the solution, constraints on the solution limit the resulting magnitude of the kinetic and potential energy.

$$\underset{\boldsymbol{\eta}_{k+1}}{\text{minimize}} \|\boldsymbol{\Phi}_{k+1}\boldsymbol{\eta}_{k+1} - \mathbf{q}_k\|_2 \quad \text{subject to} \quad \|U'_{k+1}\| \leq \|U'_k\| \tag{18}$$

$$\underset{\dot{\boldsymbol{\eta}}_{k+1}}{\text{minimize}} \|\boldsymbol{\Phi}_{k+1}\dot{\boldsymbol{\eta}}_{k+1} - \dot{\mathbf{q}}_k\|_2 \quad \text{subject to} \quad \|T'_{k+1}\| \leq \|T'_k\| \tag{19}$$

Drawbacks

The nominal LSQI approach has two primary drawbacks that inhibit its ability to effect smooth transitions. The first is that the physically realizable energy should be either equal to or less than the energy from the previous state; however, as is shown in the next section, the validity of this assumption is quite sensitive to the nature of the structure and the number of retained modes. Secondly, it does not address the homogeneous and particular solutions to the displacement independently. As a result of these issues there is potential for substantial transients across FEM model transitions, as is shown in Figures 2a and 3a.

Non-constant Energy

The basis behind the quadratically constrained approach was to enforce total system energy constant across finite element model transitions. Further investigation revealed dramatic changes in energy across transitions, especially at low mode counts seen in highly truncated FEM models. This is of significant importance because running with a large number of modes adversely impacts simulation run-time performance and it is therefore desirable to run with a reduced mode set. To better understand the discrepancy in energy between FEM models as well as the number of selected modes, the steady-state energy of the system is plotted in Figure 1 for a representative launch vehicle to visualize effects of mode count on energy across ten (10) discrete FEM models.

To estimate steady-state potential, it is assumed the structure is subject to a constant external force that has driven the system to an equilibrium state, which is a function of stiffness ($\widetilde{\mathbf{K}}$) and generalized force ($\boldsymbol{\Xi}$). Given the potential energy in Equation (16) is a function of generalized displacement ($\boldsymbol{\eta}$), the steady-state portion of generalized displacement ($\boldsymbol{\eta}_{ss}$) is found by dropping the acceleration ($\ddot{\boldsymbol{\eta}}$) and velocity ($\dot{\boldsymbol{\eta}}$) terms from Equation (20).

$$\cancel{\ddot{\boldsymbol{\eta}}_{ss}} + \mathbf{C}\cancel{\dot{\boldsymbol{\eta}}_{ss}} + \widetilde{\mathbf{K}}\boldsymbol{\eta}_{ss} = \boldsymbol{\Phi}\mathbf{f} \Rightarrow \widetilde{\mathbf{K}}\boldsymbol{\eta}_{ss} = \boldsymbol{\Xi} \tag{20}$$

$$\boldsymbol{\eta}_{ss} = \widetilde{\mathbf{K}}^{\mathbf{-1}}\boldsymbol{\Xi} \tag{21}$$

The steady-state solution ($\boldsymbol{\eta}_{ss}$) represents the particular solution (assuming constant forcing) to Equation (20), and since the stiffness ($\widetilde{\mathbf{K}}$) is known a priori and if a constant generalized force ($\boldsymbol{\Xi}$) is assumed, then the steady-state potential energy (U'_{ss}) can be calculated.

$$U'_{ss} = \boldsymbol{\eta}_{ss}^{\mathsf{T}}\widetilde{\mathbf{K}}\boldsymbol{\eta}_{ss} \tag{22}$$

Previous applications to launch vehicle flex modeling assumed sorting the modes based on modal gain placed a majority of the system energy in the first 5% to 10% of modes. However, as shown in Figure 1, this assumption does not hold, in particular when using significantly truncated mode sets. As mode count increases there is a decrease in $\Delta U'$ between mode sets, as well as a smoothing of energy between models. FEM models are unique to their specific application and the method used

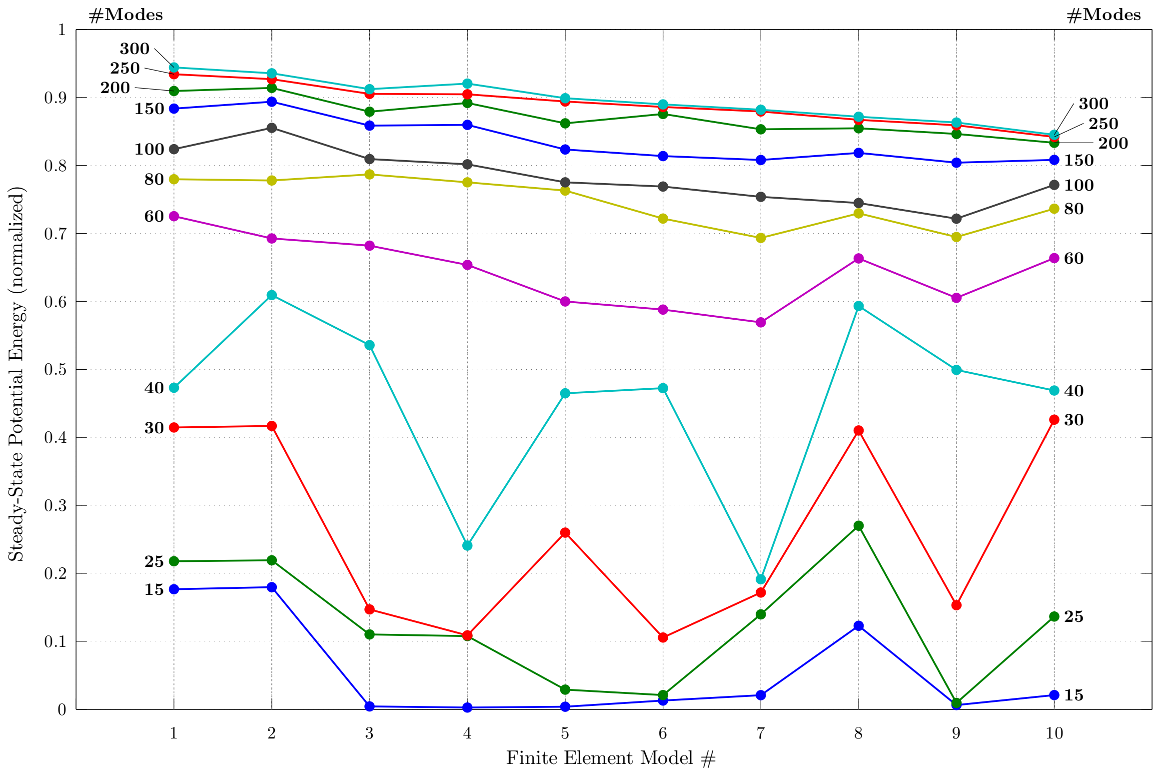

Figure 1: Equilibrium potential energy for varying mode counts across multiple FEM models

for sorting and selecting the mode set directly impacts the elastic response seen in simulation. Given the specificity of FEM models to the actual launch vehicle configuration, the analyst must visually inspect the energy discrepancy between number of selected modes and manually determine the point at which energy convergence is deemed suitable. If constant energy between models is desired, a potential method for mode selection could be based on sorting the modes based on equilibrium potential and selecting the mode set that ensures energy remains relatively constant between models. The drawback of this approach is that the time domain simulation must be capable of supporting a variable number of modes throughout the simulation and energy invariance is potentially prioritized over other important metrics, such as sensor gain.

To smooth transitions between FEM models a methodology is needed that addresses the shortcomings of previous methods by effectively handling abrupt changes in energy:

$$\boldsymbol{\eta}_k^\intercal \widetilde{\mathbf{K}}_k \boldsymbol{\eta}_k \neq \boldsymbol{\eta}_{k+1}^\intercal \widetilde{\mathbf{K}}_{k+1} \boldsymbol{\eta}_{k+1} \tag{23}$$

$$\dot{\boldsymbol{\eta}}_k^\intercal \dot{\boldsymbol{\eta}}_k \neq \dot{\boldsymbol{\eta}}_{k+1}^\intercal \dot{\boldsymbol{\eta}}_{k+1} \tag{24}$$

as well as considering the homogeneous and steady-state contributions to the total displacement.

$$\boldsymbol{\eta} = \boldsymbol{\eta}_h + \boldsymbol{\eta}_{ss} \tag{25}$$

LSQI & DIRECT SHAPE MAPPING (DSM) METHOD

To simplify the formulation, assumptions were made regarding mass matrix normalization (Equation (5)), constant external forcing ($\boldsymbol{\Xi}_k = \boldsymbol{\Xi}_{k+1}$), and constant viscous damping (Equation (8)).

These simplifications allow for direct solutions to the steady-state displacements through Direct Shape Mapping (DSM), which solves for the displacements using the natural frequencies of the elastic modes and the external forcing. For the un-forced contributions to displacement, a quadratically constrained least squares (LSQI) problem with an energy constraint is solved.

Steady-State Displacement. Thrust and aerodynamic forces constitute a substantial portion of the total launch vehicle system energy and appear primarily as potential energy in the system, and greatly exceed the kinetic energy in the structure, $U' \gg T'$. Equation (20) presents the simplifications exercised to compute the steady-state portion of generalized displacement ($\boldsymbol{\eta}_{ss}$), which is strictly a function of modal stiffness ($\widetilde{\mathbf{K}}$) and generalized force ($\boldsymbol{\Xi}$), as shown in Equation (21). Since the external force is substantial compared to other forces on the launch vehicle, it is important to accurately calculate ($\boldsymbol{\eta}_{ss}$) to properly capture the forcing contribution. Given the modal frequencies (ω_n^2) are known a priori and the generalized force ($\boldsymbol{\Xi}$) is assumed constant across transitions ($\boldsymbol{\Xi}_k = \boldsymbol{\Xi}_{k+1}$), it is possible to solve directly for the steady-state portion of the displacement ($\boldsymbol{\eta}_{ss}$) given the future FEM model.

$$\boldsymbol{\eta}_{ss_{k+1}} = \widetilde{\mathbf{K}}_{k+1}^{-1}\boldsymbol{\Xi}_{\mathbf{k}} = \widetilde{\mathbf{K}}_{k+1}^{-1}(\boldsymbol{\Phi}_{k+1}\mathbf{f}_{\mathbf{k}}) \tag{26}$$

This approach is labeled Direct Shape Matching (DSM) as the generalized displacement following the transition ($\boldsymbol{\eta}_{ss_{k+1}}$) is directly mapped to the equilibrium displacement.

Homogeneous Displacement. For the homogeneous solution, Equation (10) is set equal to zero:

$$\ddot{\boldsymbol{\eta}}_h + \mathbf{C}\dot{\boldsymbol{\eta}}_h + \widetilde{\mathbf{K}}\boldsymbol{\eta}_h = 0 \tag{27}$$

Contrary to the steady-state solution which is a function of the generalized force ($\boldsymbol{\Xi}$), the homogeneous solution is a function solely of the damping ($\mathbf{C}$) and stiffness ($\widetilde{\mathbf{K}}$). Assuming $\zeta \ll 1$ the homogeneous solution can be approximated as a function of only stiffness. To form the constraints for the least squares problem, the steady-state displacement from the initial FEM model ($\boldsymbol{\eta}_{ss_k}$) is needed to find the homogeneous displacement ($\boldsymbol{\eta}_{h_k}$) from the same model.

$$\boldsymbol{\eta}_{ss_k} = \widetilde{\mathbf{K}}_k^{-1}\boldsymbol{\Xi}_k = \widetilde{\mathbf{K}}_k^{-1}(\boldsymbol{\Phi}_k\mathbf{f}_{\mathbf{k}}) \tag{28}$$

$$\boldsymbol{\eta}_{h_k} = \boldsymbol{\eta}_k - \boldsymbol{\eta}_{ss_k} \tag{29}$$

The homogeneous displacement is then used to calculate the potential energy due to the homogeneous portion of the solution, which is then used as a constraint when solving for $\boldsymbol{\eta}_{h_{k+1}}$.

$$U'_{h_k} = \boldsymbol{\eta}_{h_k}^{\mathsf{T}}\widetilde{\mathbf{K}}_k\boldsymbol{\eta}_{h_k} \qquad U'_{h_{k+1}} = \boldsymbol{\eta}_{h_{k+1}}^{\mathsf{T}}\widetilde{\mathbf{K}}_{k+1}\boldsymbol{\eta}_{h_{k+1}}$$

The least squares problem can now be solved using the potential energy constraints.

$$\underset{\boldsymbol{\eta}_{h_{k+1}}}{\text{minimize}}\|\boldsymbol{\Phi}_{k+1}\boldsymbol{\eta}_{h_{k+1}} - (\mathbf{q}_k - \mathbf{q}_{ss_k})\|_2 \quad \text{subject to} \quad \|U'_{h_{k+1}}\| \leq \|U'_{h_k}\| \tag{30}$$

Total Displacement. The total displacement $\boldsymbol{\eta}_{k+1}$ can now be found as the superposition of the steady-state displacement ($\boldsymbol{\eta}_{ss_{k+1}}$) and the homogeneous displacement ($\boldsymbol{\eta}_{h_{k+1}}$):

$$\boldsymbol{\eta}_{k+1} = \boldsymbol{\eta}_{h_{k+1}} + \boldsymbol{\eta}_{ss_{k+1}} \tag{31}$$

Velocity. When solving for the generalized velocity ($\dot{\boldsymbol{\eta}}_{k+1}$) the external forcing ($\boldsymbol{\Xi}$) is ignored because a constant force only directly impacts displacement ($\boldsymbol{\eta}$). Since external forcing only directly impacts displacement ($\boldsymbol{\eta}$) and potential (U'), the kinetic energy (T') can be solved for without consideration of the generalized force ($\boldsymbol{\Xi}$).

$$T'_k = \dot{\boldsymbol{\eta}}_k^\intercal \dot{\boldsymbol{\eta}}_k \qquad T'_{k+1} = \dot{\boldsymbol{\eta}}_{k+1}^\intercal \dot{\boldsymbol{\eta}}_{k+1}$$

In a manner identical to the LSQI method, the generalized velocity ($\dot{\boldsymbol{\eta}}_{k+1}$) is now solved for as a least squares problem with a kinetic energy constraint.

$$\underset{\dot{\boldsymbol{\eta}}_{k+1}}{\text{minimize}} \|\boldsymbol{\Phi}_{k+1}\dot{\boldsymbol{\eta}}_{k+1} - \dot{\mathbf{q}}_k\|_2 \quad \text{subject to} \quad \|T'_{k+1}\| \leq \|T'_k\| \tag{32}$$

ANALYSIS OF LSQI-DSM METHOD

LSQI-DSM was analyzed using NASA's Space Launch System (SLS) vehicle time domain simulation tool, MAVERIC (Marshall Aerospace Vehicle Representation in C). To ensure that transients at FEM model transitions were reduced, energy was neither added or removed from that dictated by each FEM model. The effects of excitation at vehicle transitions on the control system performance were analyzed, and test cases were developed to excite the system over multiple FEM model transitions so as to evaluate the effectiveness of the LSQI-DSM method.

Removal of transients

In this application, a standalone LSQI approach produces appreciable transients following FEM model transitions. Truncation of the mode set invalidates the constant energy assumption between models and therefore methods expecting constant energy will not produce smooth transitions. In addition, omission of the forced response in the solution to Equation (10) results in poorly conditioned initial states at the start of each FEM model, producing severe excitation as shown in Figures 2a and 3a, which display the system total energy and sensed acceleration due to elastic motion. The data reflects a portion of total flight time and details the first five (5) transitions in a simulation.

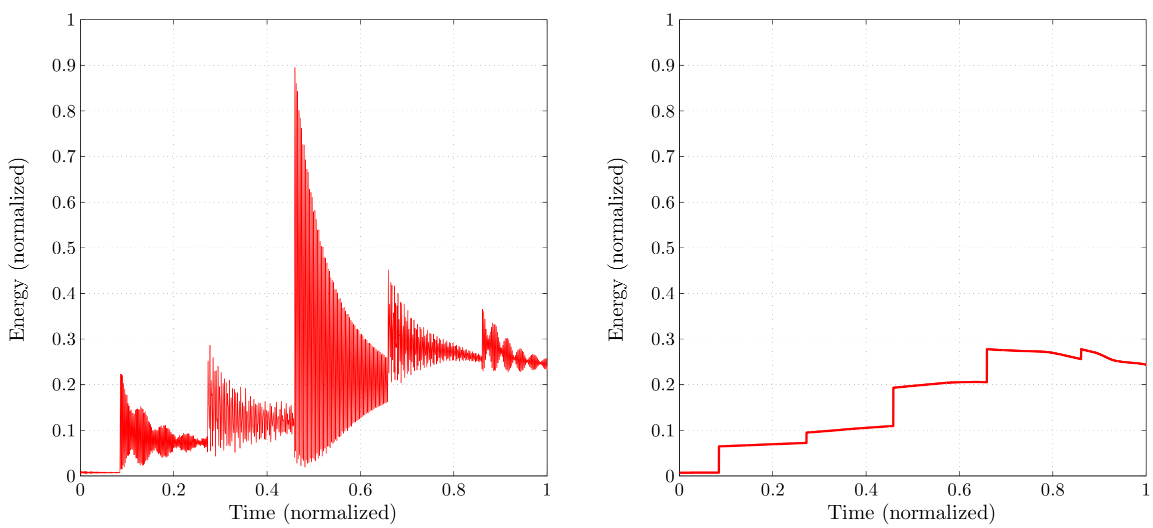

(a) Nominal LSQI

(b) LSQI-DSM

Figure 2: LSQI versus LSQI-DSM and the effect on energy following FEM model transitions

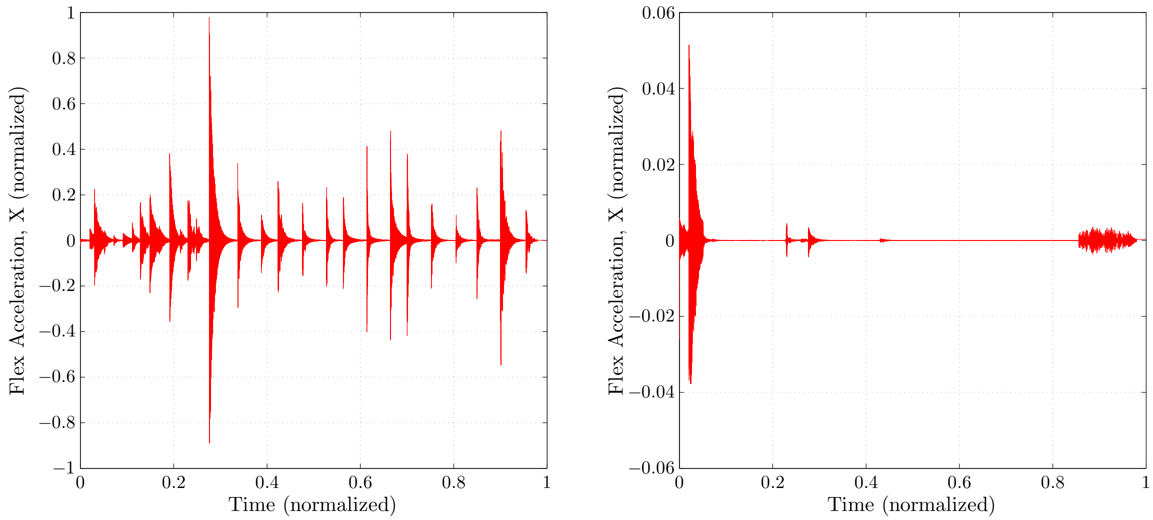

(a) Nominal LSQI

(b) LSQI-DSM

Figure 3: LSQI versus LSQI-DSM and the effects on sensed acceleration

In comparison, Figures 2b and 3b highlight the results using the LSQI-DSM method which shows improvements ranging from a significant reduction to a complete removal of transients, except for cases involving external excitation.

Verification of energy conservation

Verification of the LSQI-DSM method was performed by examining elastic motion in the vicinity of FEM model transitions. The test case used a sinusoidal force tuned to the first three bending mode frequencies and was applied to the system via a force input grid on the vehicle. Intended to provide sufficient excitation to oscillate the structure over multiple model transitions, the goal was to evaluate LSQI-DSM performance without controller interaction. The test case provides comparison of pure DSM, LSQI-DSM, and free decay of the system after being subjected to the sinusoidal input. Transitions were disabled to allow estimation of free-decay in the system, while the DSM and LSQI-DSM cases were allowed to perform transitions as designed.

The free-decay case is intended to serve as a benchmark that demonstrates elastic behavior in the absence of FEM model model transitions. Figure 4a details the potential and kinetic energies as defined by Equations (16) and (17), and highlights the dominance of potential energy in the overall system. In the vicinity of the sinusoidal test input, kinetic energy shown in Figure 4b exhibits a small amplitude decrease for both DSM and LSQI-DSM; however, LSQI-DSM sustains more residual kinetic energy across the transition. For potential energy, Figure 4c details the response for all three cases, and Figure 4d provides additional evidence of LSQI-DSM's ability to sustain energy across multiple transitions. For all tests performed, the input force free decay time is consistent.

Immediately following FEM model transitions, LSQI-DSM sustains kinetic energy across multiple transitions and shows a decay rate equivalent to that of the free-decay. Preservation of the elastic motion and natural decay of the motion is validation that LSQI-DSM is not artificially adding or removing kinetic energy. Investigation of the potential energy provides similar conclusions, and shows that smooth transition of the potential energy is maintained and is still present two transitions following the excitation, meanwhile the DSM method truncates the potential energy.

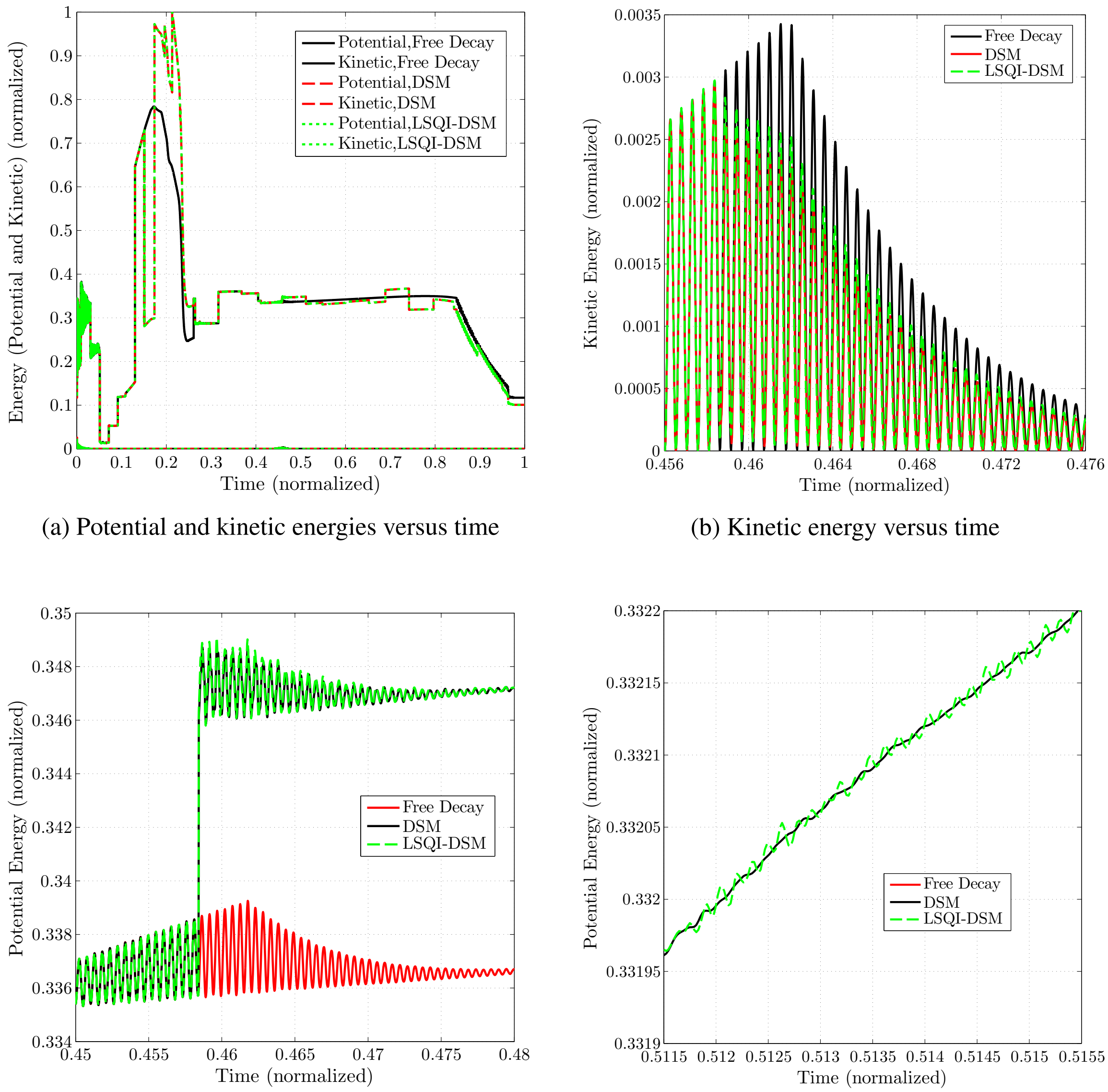

(a) Potential and kinetic energies versus time

(b) Kinetic energy versus time

(c) Potential energy snapshot 1

(d) Potential energy snapshot 2

Figure 4: Comparison of various methods and the preservation of elastic motion across transitions

Impact to vehicle control design

The SLS control architecture uses an adaptive controller[9] to reduce total controller gain if undesirable control-structure interactions are detected. With the previous LSQI method, elastic dynamics induced at FEM model transitions were sensed by the adaptive controller and interpreted as structural instability, leading to a decrease in loop gain. This behavior is undesirable as excitation at the model transition is artificial. The LSQI-DSM method reduces/completely removes the artificial transient and in turn reduces the controller response to the excitation, as shown in Figures 5a and 5b.

A drawback of LSQI-DSM when compared to the previous LSQI implementation is discontinuity in the physical displacements immediately following a transition. Discontinuity in physical states

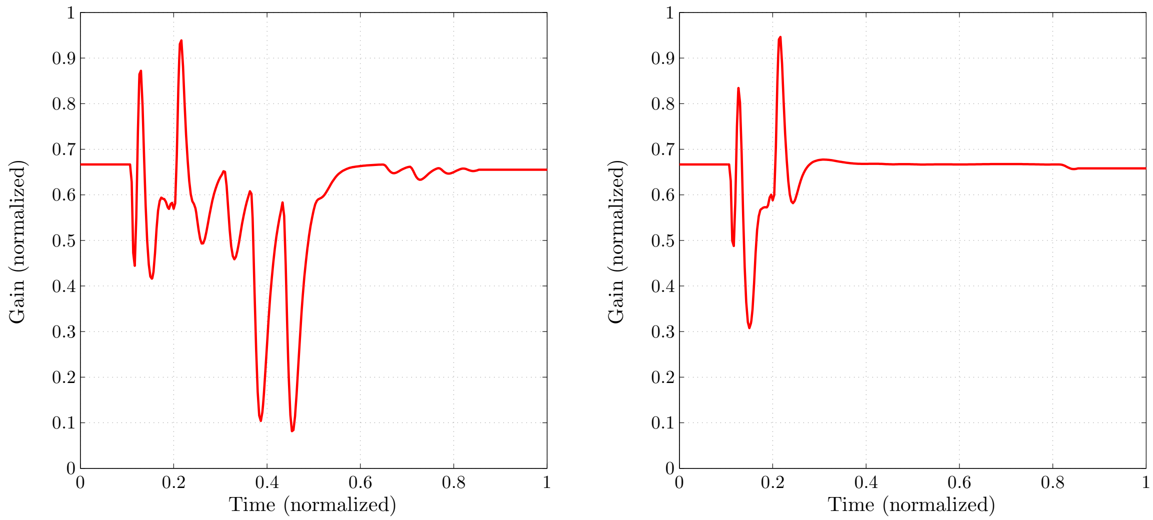

(a) Nominal LSQI

(b) LSQI-DSM

Figure 5: Positive impact on system total loop gain

coupled with the vehicle rigid body motion produces a discontinuous kinematic solution, which in the presence of inertial navigation, can produce large inertial errors. To solve this problem, consideration must be given in the simulation to ensure kinematic continuity across transitions.

CONCLUSION

In order to aid in the time domain evaluation, analysis, and verification of launch vehicle control system design, a technique to transition between multiple LTI FEM models has been demonstrated. The proposed LSQI-DSM method offers appreciable improvements over prior methods by addressing non-constant energy that is experienced when employing a truncated mode set in simulations intended to stress specific modes of importance to the control design activities. The LSQI-DSM approach accommodates large changes in system energy between FEM models perpetuated by the use of a truncated mode set, and shows significant reduction or complete removal of non-physical transients, as well as sustaining elastic motion across FEM model transitions.

ACKNOWLEDGMENT

The authors would like to thank Jeb Orr of Draper Laboratory for his insight, knowledge, and substantial contributions to this paper. Research and development of the LSQI-DSM method was performed under contract NNM12AA41C.

NOTATION

$[\ ]_k$	any variable where subscript "$_k$" indicates the current finite element model
$[\ ]_{k+1}$	any variable where subscript "$_{k+1}$" indicates the subsequent finite element model
$[\ ]_{ss}$	steady-state component of the parent variable
$[\ ]_h$	homogeneous component of the parent variable
E	total energy
U	potential energy

T	kinetic energy
U'	potential energy using truncated mode set
T'	kinetic energy using truncated mode set
$\boldsymbol{q}$	physical displacement
$\dot{\boldsymbol{q}}$	physical velocity
$\ddot{\boldsymbol{q}}$	physical acceleration
$\boldsymbol{\eta}$	generalized displacement
$\dot{\boldsymbol{\eta}}$	generalized velocity
$\ddot{\boldsymbol{\eta}}$	generalized acceleration
$\boldsymbol{I}$	identity matrix
$\boldsymbol{M}$	mass matrix
$\boldsymbol{K}$	stiffness matrix
$\widetilde{\boldsymbol{K}}$	diagonal stiffness matrix
$\boldsymbol{C}$	damping matrix
$\boldsymbol{f}$	excitation forces and torques
$\boldsymbol{\Xi}$	generalized force
$\boldsymbol{\Phi}$	eigenvectors of the elastic modes
i	mode number
m	maximum number of modes
ω_n^2	natural frequencies of the of elastic modes
ζ	damping ratio

REFERENCES

[1] J. Orr, "Elastic Model Transitions Using Quadratic Inequality Constrained Least Squares," *AIAA Atmospheric Flight Mechanics Conference*, Toronto, CA, 2010. AIAA-2010-7642.

[2] J. Zapico-Valle, R. Alonso-Camblor, M. González-Martínez, and M. García-Diéguez, "A new method for finite element model updating in structural dynamics," *Mechanical Systems and Signal Processing*, 2010, pp. 2137–2159.

[3] J. Mottershead and M. Friswell, "Model Updating in Structural Dynamics: A Survey," *Journal of Sound and Vibration 167(2)*, 1993, pp. 347–375.

[4] A. Berman and E. Nagy, "Improvements of a Large Analytical Model Using Test Data," *Proceedings of the 23rd AIAA/ASME/ASCE/AHS Structures, Structural Dynamics and Materials Conference*, May 1982. Paper 82-0743.

[5] Y. Yang, Y. Chen, and T. Hsu, "Direct Updating Method for Structural Models Based on Orthogonality Constraints," *Mechanics of Advanced Materials and Structures*, Taylor & Francis, 2009, pp. 390–401.

[6] B. Jaishi and W. Ren, "Damage detection by finite element model updating using modal flexibility residual," *Journal of Sound and Vibration 290*, 2006, pp. 347–375.

[7] A. Kabe, "Mode Shape Identification and Orthogoanlization," *Proceedings of the 29th AIAA/ASME/ASCE/AHS Structures, Structural Dynamics and Materials Conference*, May 1988. Paper 88-2354.

[8] D. Hodges and G. Pierce, *Introduction to Structural Dynamics and Aeroelasticity*. New York, NY: Cambrudge University Press, 2005.

[9] J. Orr and T. VanZwieten, "Robust, Practical Adaptive Control for Launch Vehicles," August 2012. AIAA-2012-15662.

SLS

Space Launch System

Elastic Model Transitions:

A Hybrid Approach Utilizing Quadratic Inequality Constrained Least Squares (LSQI) and Direct Shape Matching (DSM)

Robert Jurenko *(Leidos Inc. / Jacobs ESSSA)*
Jason Bush *(Tri-Vector Services Inc. / Jacobs ESSSA)*
John Ottander *(Dynamic Concepts Inc. / Jacobs ESSSA)*

AAS 14-304

December 16, 2013

Outline

- Summary
  - *Simulation of launch vehicle elastic behavior*
  - *Previous approaches to transitioning between FEM models*
  - *Drawbacks and identification of solution path*
- Formulation of the Theory
  - *Equations of Motion in generalized coordinates*
  - *Formulation of energy constraints*
- Nominal LSQI Method
  - *LSQI method drawbacks*
- Non-Constant Energy
- LSQI-DSM Method
  - *Steady-state solution*
  - *Homogeneous solution*
  - *Total displacement*
- Results
  - *Analysis of LSQI-DSM method*
  - *Removal of transients*
  - *Verification of energy conservation*
  - *Impact to vehicle control design*
- Conclusion
- Acknowledgments

Summary

The time invariant nature of elastic data in launch vehicle simulations poses the problem:

How to properly transition elastic states between finite element models while preserving motion across the transition

- **A method for transitioning linear time invariant (LTI) models in time varying simulation is proposed that utilizes:**
  - Quadratically constrained least squares (LSQI) and
  - Direct Shape Mapping (DSM)
- **LSQI-DSM applies to the simulation of the elastic behavior of launch vehicles and other structures that utilize multiple discrete finite element model (FEM) derived mode sets**
- **LSQI-DSM algorithm designed to handle truncated mode sets:**
  - Can accommodate significant changes in energy across FEM models
  - Ensures flex motion across model transitions

Background

- **Launch vehicle controller design considers the elastic behavior of the system as it directly impacts sensor feedback and controller performance**
- **Simulation of launch vehicle elastic behavior is traditionally accomplished using multiple FEM models:**
  - Models provided at set intervals throughout flight
  - Models correspond to vehicle mass & stiffness
  - Typically provided every 10 to 20 seconds of flight time, for which the models are held fixed until conditions reached for next model
- **Dissimilarities between FEM models requires a transition method that:**
  - Captures existing flex motion of the system
  - Does not introduce non-physical displacement, velocity, or acceleration to the system (i.e. ringing)

Background

- **Computational burden of propagating a large number of modes in a launch vehicle simulation is significant:**
  - Subset of modes is typically selected to reduce run time
- **Using a truncated FEM model can result in:**
  - Non-constant energy between models
  - Transients immediately following model transition due to poorly conditioned initial conditions
- **The problem to be solved:**
  - Given a known set of physical bending displacements and velocities at time t_0, what set of new generalized coordinates optimally approximates the physical coordinates using a new basis at t_1 [1]

Background

- **In search of a physically realistic way to transition between models, an approach based on Quadratic Inequality Constrained Least Squares (LSQI) [1] was developed to effect a smooth transition between models**
  - By way of an energy constraint, the LSQI algorithm uses the eigenvectors of the future state (Φ_{k+1}) and prior physical state (Φ_k) to estimate generalized coordinates ($\boldsymbol{\eta}$, $\dot{\boldsymbol{\eta}}$) that result in an overall system energy at or below the prior energy level
  - Key benefits of this method include no requirement that the models be of similar dimension, or that the eigenvectors be correlated in any way

Background

- **Simulation results show that while LSQI ensures constant energy across a transition, $U'_k = U'_{k+1}$, non-physical transients "ring" the system at FEM model transitions**

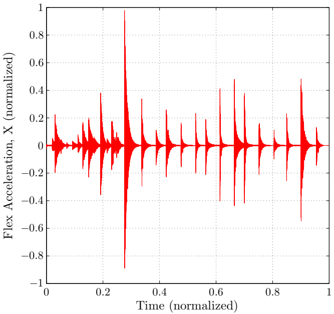

Figure 1: Nominal LSQI

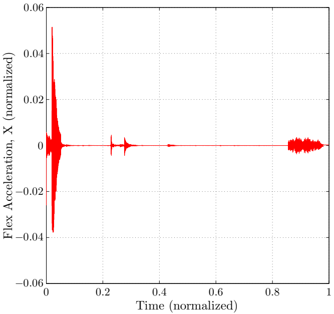

Figure 2: LSQI-DSM

- **An explanation was sought to determine the cause of the transients at transition points**

- **Two primary causes were identified:**

  1. Running with a truncated mode set invalidates the assumption that energy is approximately constant across transitions

$$\boldsymbol{\eta}_k^\intercal \widetilde{\mathbf{K}}_k \boldsymbol{\eta}_k \neq \boldsymbol{\eta}_{k+1}^\intercal \widetilde{\mathbf{K}}_{k+1} \boldsymbol{\eta}_{k+1} \tag{1}$$

$$\dot{\boldsymbol{\eta}}_k^\intercal \dot{\boldsymbol{\eta}}_k \neq \dot{\boldsymbol{\eta}}_{k+1}^\intercal \dot{\boldsymbol{\eta}}_{k+1} \tag{2}$$

  2. Fixing the physical displacement and velocity across transitions while abruptly changing stiffness & damping excites the system

$$\underset{\boldsymbol{\eta}_{k+1}}{\text{minimize}} \|\boldsymbol{\Phi}_{k+1}\boldsymbol{\eta}_{k+1} - \mathbf{q}_k\|_2 \quad \text{s.t.} \quad \|U'_{k+1}\| \leq \|U'_k\| \tag{3}$$

$$\underset{\dot{\boldsymbol{\eta}}_{k+1}}{\text{minimize}} \|\boldsymbol{\Phi}_{k+1}\dot{\boldsymbol{\eta}}_{k+1} - \dot{\mathbf{q}}_k\|_2 \quad \text{s.t.} \quad \|T'_{k+1}\| \leq \|T'_k\| \tag{4}$$

Formulation of the Theory

- **The size and complexity of complete FEM models requires a computationally efficient transition methodology**
  - The LSQI approach[1] and LSQI-DSM represent efficient approaches to updating the FEM model data throughout the launch vehicle time-domain simulation
- **Given a priori knowledge of the stiffness ($\mathbb{K}$), damping ($\mathbb{C}$), and eigenvectors (Φ) from the launch vehicle finite element model, the goal is:**
  - To effect a smooth transition between these models
  - Solve for physical/generalized states following model transition
  - Preserves elastic motion across the transition

Formulation of the Theory

- **The undamped motion is described by:**

$$\mathbf{M}\ddot{\mathbf{q}} + \mathbf{K}\mathbf{q} = \mathbf{f} \tag{5}$$

- **where $\mathbf{M}$ is the mass matrix, $\mathbf{K}$ is the stiffness matrix, $\mathbf{f}$ is a vector of excitation forces and torques, and $\mathbf{q}$ is a vector of displacements in physical coordinates**

- **To transform from physical to generalized coordinates the following substitutions are made:**

$$\mathbf{q} = \boldsymbol{\Phi}\boldsymbol{\eta} \qquad \dot{\mathbf{q}} = \boldsymbol{\Phi}\dot{\boldsymbol{\eta}} \tag{6}$$

- **Equation (5) can now be written in generalized coordinates**

$$\mathbf{M}\boldsymbol{\Phi}\ddot{\boldsymbol{\eta}} + \mathbf{K}\boldsymbol{\Phi}\boldsymbol{\eta} = \mathbf{f} \tag{7}$$

Formulation of the Theory

- **Multiplying by the transpose provides:**

$$\mathbf{\Phi}^{\mathsf{T}}\mathbf{M}\mathbf{\Phi}\ddot{\boldsymbol{\eta}} + \mathbf{\Phi}^{\mathsf{T}}\mathbf{K}\mathbf{\Phi}\boldsymbol{\eta} = \mathbf{\Phi}^{\mathsf{T}}\mathbf{f} \tag{8}$$

- **The eigenvector matrix ($\mathbf{\Phi}$) is selected to satisfy:**
  - $\mathbf{\Phi}^{\mathsf{T}}\mathbf{M}\mathbf{\Phi} = \mathbf{I}$
  - $\mathbf{\Phi}^{\mathsf{T}}\mathbf{K}\mathbf{\Phi} = \text{diag}(\omega_n^2)$
  - and the orthonormality constraint

- **Constant viscous damping is assumed**

$$\widetilde{\mathbf{K}} = \begin{pmatrix} \omega_{n_1}^2 & 0 & \dots & 0 \\ 0 & \omega_{n_2}^2 & \dots & 0 \\ \vdots & \vdots & \ddots & \vdots \\ 0 & 0 & \dots & \omega_{n_k}^2 \end{pmatrix} \quad \mathbf{C} = \begin{pmatrix} 2\zeta\omega_{n_1} & 0 & \dots & 0 \\ 0 & 2\zeta\omega_{n_2} & \dots & 0 \\ \vdots & \vdots & \ddots & \vdots \\ 0 & 0 & \dots & 2\zeta\omega_{n_k} \end{pmatrix}$$

Formulation of the Theory

- **The generalized force represents effective loading of all forces & moments on the launch vehicle:**

$$\boldsymbol{\Xi} = \boldsymbol{\Phi}^{\mathsf{T}}\mathbf{f} \tag{9}$$

- **Given transformation** (6) **and prior assumptions, Equation 8 can be rewritten as:**

$$\ddot{\boldsymbol{\eta}} + \mathbf{C}\dot{\boldsymbol{\eta}} + \widetilde{\mathbf{K}}\boldsymbol{\eta} = \boldsymbol{\Xi} \tag{10}$$

- **The least squares problem is bounded by:**
  - Potential energy constraint on the generalized displacement ($\boldsymbol{\eta}$)
  - Kinetic energy constraint on the generalized velocity ($\dot{\boldsymbol{\eta}}$)

- **Recap, total displacement can be written as sum of all modal contributions**

$$q = \sum_{i=1}^{\infty} \boldsymbol{\Phi}_i \boldsymbol{\eta}_i \tag{11}$$

Formulation of the Theory

- **Similarly, total potential & kinetic energy are found by summing modal contributions**
- **Using transformation** (6) **& earlier assumptions, energy can be expressed in generalized coordinates:**

$$U = \frac{1}{2}\sum_{i}^{\infty}\mathbf{K}_{i,i}\mathbf{q}_i^2 = \frac{1}{2}\sum_{i}^{\infty}\widetilde{\mathbf{K}}_{i,i}\boldsymbol{\eta}_i^2 \tag{12}$$

$$T = \frac{1}{2}\sum_{i}^{\infty}\mathbf{M}_{i,i}\dot{\mathbf{q}}_i^2 = \frac{1}{2}\sum_{i}^{\infty}\mathbf{I}_{i,i}\dot{\boldsymbol{\eta}}_i^2 \tag{13}$$

- **Equations** (12) **and** (13) **represent total kinetic and potential energy assuming an infinitely large mode set**
- **For simulation purposes, the maximum number of modes,** m**, is a finite quantity**

Formulation of the Theory

- **The corresponding "total" potential and kinetic energies are in reality only a portion of the total physical quantities**
- **Hereinafter, use of "total kinetic" and "total potential" will refer to the total potential (U') and kinetic (T') prescribed by the truncated mode set.**

$$U' = \frac{1}{2}\sum_{i}^{m}\mathbf{K}_{i,i}\mathbf{q}_i^2 = \frac{1}{2}\sum_{i}^{m}\widetilde{\mathbf{K}}_{i,i}\boldsymbol{\eta}_i^2 \tag{14}$$

$$T' = \frac{1}{2}\sum_{i}^{m}\mathbf{M}_{i,i}\dot{\mathbf{q}}_i^2 = \frac{1}{2}\sum_{i}^{m}\mathbf{I}_{i,i}\dot{\boldsymbol{\eta}}_i^2 \tag{15}$$

- **Equations** (14) **and** (15) **can be written as a quadratic form.**

$$U' = \boldsymbol{\eta}^{\mathsf{T}}\widetilde{\mathbf{K}}\boldsymbol{\eta} \tag{16}$$

$$T' = \dot{\boldsymbol{\eta}}^{\mathsf{T}}\dot{\boldsymbol{\eta}} \tag{17}$$

LSQI Method

- **Basis functions between FEM models not equal $\mathbf{\Phi_k \neq \Phi_{k+1}}$**
- **A method is required to calculate the displacement (η_{k+1}) and velocity ($\dot{\eta}_{k+1}$) given the subsequent FEM model**
- **To bound the solution, constraints on the solver limit the resulting magnitude of the kinetic and potential energy**

$$\underset{\boldsymbol{\eta}_{k+1}}{\text{minimize}} \|\boldsymbol{\Phi}_{k+1}\boldsymbol{\eta}_{k+1} - \mathbf{q}_k\|_2 \quad \text{s.t.} \quad \|U'_{k+1}\| \leq \|U'_k\| \tag{18}$$

$$\underset{\dot{\boldsymbol{\eta}}_{k+1}}{\text{minimize}} \|\boldsymbol{\Phi}_{k+1}\dot{\boldsymbol{\eta}}_{k+1} - \dot{\mathbf{q}}_k\|_2 \quad \text{s.t.} \quad \|T'_{k+1}\| \leq \|T'_k\| \tag{19}$$

LSQI Method Drawbacks

- **The original LSQI approach has two key drawbacks that generate excitation across FEM model transitions:**
  1. Assumes energy approximately constant across transition
  2. Does not separately address homogeneous & particular solutions

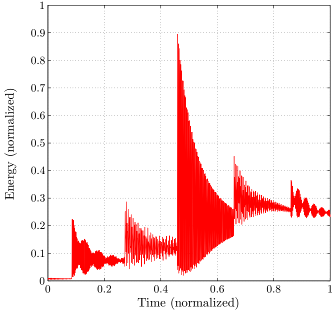

Figure 3: Nominal LSQI

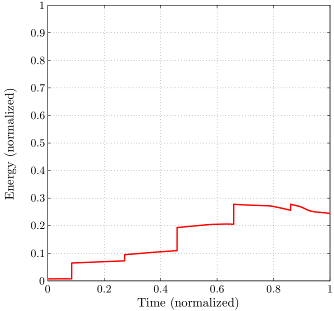

Figure 4: LSQI-DSM

Non-Constant Energy

- **Investigation of FEM models revealed dramatic changes in energy across transitions**

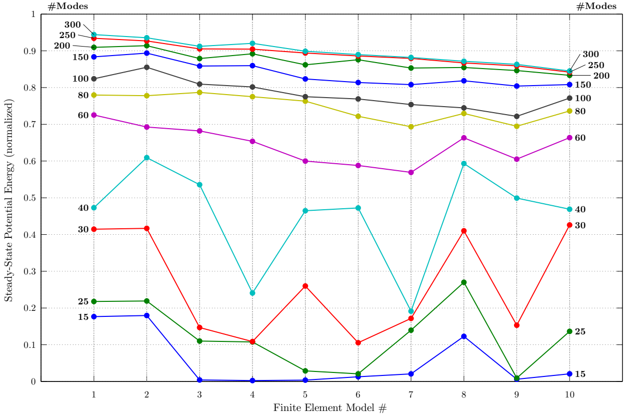

Figure 5: Equilibrium potential energy for varying mode counts

Non-Constant Energy

- **Previous applications to launch vehicle flex modeling assumed sorting the modes based on modal gain**
- **FEM models are unique to their specific applications, therefore the analyst must visually inspect and manually determine the point of energy convergence**
- **To provide smooth transitions, a methodology is needed that can handle abrupt changes in energy:**

$$\boldsymbol{\eta}_k^{\mathsf{T}} \widetilde{\mathbf{K}}_k \boldsymbol{\eta}_k \neq \boldsymbol{\eta}_{k+1}^{\mathsf{T}} \widetilde{\mathbf{K}}_{k+1} \boldsymbol{\eta}_{k+1} \tag{20}$$

$$\dot{\boldsymbol{\eta}}_k^{\mathsf{T}} \dot{\boldsymbol{\eta}}_k \neq \dot{\boldsymbol{\eta}}_{k+1}^{\mathsf{T}} \dot{\boldsymbol{\eta}}_{k+1} \tag{21}$$

- **This method must also address both the homogeneous & steady-state solutions to the total displacement**

$$\boldsymbol{\eta} = \boldsymbol{\eta}_h + \boldsymbol{\eta}_{ss} \tag{22}$$

Direct Shape Mapping (DSM)

- **Thrust & aerodynamic forces constitute a substantial portion of system energy**
- **These forces appear in the potential energy and greatly outweigh the kinetic energy of the structure, $U' \gg T'$**
- **Given the potential energy in Equation (16) is a function of generalized displacement (η), the steady-state contribution of generalized displacement (η_{ss}) is found by dropping the acceleration and velocity terms:**

$$\cancel{\ddot{\eta}_{ss}} + \mathbf{C}\cancel{\dot{\eta}_{ss}} + \widetilde{\mathbf{K}}\eta_{ss} = \mathbf{\Phi f} \rightarrow \widetilde{\mathbf{K}}\eta_{ss} = \mathbf{\Xi} \qquad (23)$$

Direct Shape Mapping (DSM)

- The steady-state displacement η_{ss} is strictly a function of stiffness ($\widetilde{\mathrm{K}}$) and force (Ξ)
- Given the modal frequencies ω_n^2 are known a priori and the generalized force Ξ is assumed constant across transitions:

$$\Xi_k = \Xi_{k+1} \tag{24}$$

steady-state displacement can be solved directly:

$$\eta_{ss_{k+1}} = \widetilde{\mathbf{K}}_{k+1}^{-1} \Xi_k \tag{25}$$

- This this approach is labeled Direct Shape Matching (DSM) as the generalized displacements are directly mapped to the equilibrium displacement governed by Φ_{k+1}, $\omega_{n_{k+1}}$, and Ξ_k

LSQI-DSM

- **Homogeneous solution** $\rightarrow$ **Equation** (10) **set equal to zero:**
  - Function solely of damping ($\mathbf{C}$) and stiffness ($\widetilde{\mathbf{K}}$).
  - Assuming $\zeta \ll 1$ the homogeneous solution can be approximated as a function of only stiffness

$$\ddot{\boldsymbol{\eta}}_h + \mathbf{C}\dot{\boldsymbol{\eta}}_h + \widetilde{\mathbf{K}}\boldsymbol{\eta}_h = 0 \tag{26}$$

- **To form the constraints for LSQI, the steady-state displacement from the initial FEM model (η_{ss_k}) is needed to find the homogeneous portion of the displacement (η_{h_k})**

$$\boldsymbol{\eta}_{ss_k} = \widetilde{\mathbf{K}}_k^{-1}\boldsymbol{\Xi}_k = \widetilde{\mathbf{K}}_k^{-1}(\boldsymbol{\Phi}_k \mathbf{f}_k) \tag{27}$$

$$\boldsymbol{\eta}_{h_k} = \boldsymbol{\eta}_k - \boldsymbol{\eta}_{ss_k} \tag{28}$$

LSQI-DSM

- **The homogeneous displacement is used to calculate the homogeneous portion of potential energy**

$$U'_{h_k} = \boldsymbol{\eta}_{h_k}^{\mathsf{T}} \widetilde{\mathbf{K}}_k \boldsymbol{\eta}_{h_k} \tag{29}$$

$$U'_{h_{k+1}} = \boldsymbol{\eta}_{h_{k+1}}^{\mathsf{T}} \widetilde{\mathbf{K}}_{k+1} \boldsymbol{\eta}_{h_{k+1}} \tag{30}$$

- **The least squares problem is now solved subject to the energy constraints:**

$$\underset{\dot{\boldsymbol{\eta}}_{h_{k+1}}}{\text{minimize}} \|\boldsymbol{\Phi}_{k+1}\boldsymbol{\eta}_{h_{k+1}} - (\mathbf{q}_k - \mathbf{q}_{ss_k})\|_2 \quad \text{s.t.} \quad \|U'_{h_{k+1}}\| \leq \|U'_{h_k}\| \tag{31}$$

- **Total displacement η is the superposition of steady-state and homogeneous solutions:**

$$\boldsymbol{\eta}_{k+1} = \boldsymbol{\eta}_{h_{k+1}} + \boldsymbol{\eta}_{ss_{k+1}} \tag{32}$$

LSQI-DSM

- **When solving for generalized velocity ($\dot{\eta}_{k+1}$) the external forcing is ignored**
  - Constant forcing only directly impacts displacement ($\boldsymbol{\eta}$)
  - Kinetic energy solved without consideration of generalized force

$$T'_k = \dot{\boldsymbol{\eta}}_k^{\mathsf{T}} \dot{\boldsymbol{\eta}}_k \qquad T'_{k+1} = \dot{\boldsymbol{\eta}}_{k+1}^{\mathsf{T}} \dot{\boldsymbol{\eta}}_{k+1} \tag{33}$$

- **Similar to nominal LSQI, generalized velocity is solved as a least squares problem with a kinetic energy constraint**

$$\underset{\dot{\boldsymbol{\eta}}_{k+1}}{\text{minimize}} \|\boldsymbol{\Phi}_{k+1}\dot{\boldsymbol{\eta}}_{k+1} - \dot{\mathrm{q}}_k\|_2 \quad \text{s.t.} \quad \|T'_{k+1}\| \leq \|T'_k\| \tag{34}$$

Analysis of LSQI-DSM Method

- **LSQI-DSM was evaluated using MAVERIC (Marshall Aerospace Vehicle Representation in C)**
- **Two problems drove excitation in LSQI approach:**
  - Truncated mode set invalidates constant energy assumption
  - Omission of forced response in the displacement solution resulted in poorly conditioned initial states at the start of each FEM model
- **LSQI-DSM method addressed these two issues by:**
  - Using DSM to initialize the forced response
  - Using the LSQI approach to capture the un-forced response
  - Total solution is a combination of forced & un-forced solutions

Removal of Transients

- **LSQI-DSM shows improvements ranging from a significant reduction to a complete removal of transients, except for cases involving external excitation**
- **In case of energy, LSQI-DSM transitions without excitation**

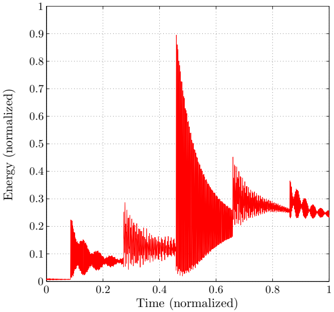

Figure 6: LSQI

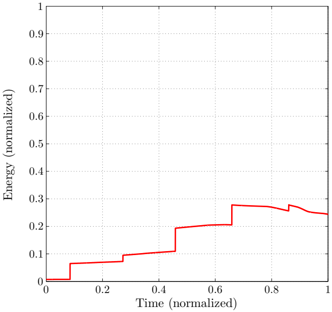

Figure 7: LSQI-DSM

Removal of Transients

- **In case of sensed acceleration, LSQI-DSM significantly reduces excitation, which has:**
  - Positive impact on sensor output
  - Leads to reduced error in navigation solution

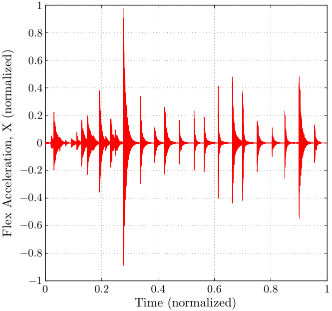

Figure 8: LSQI

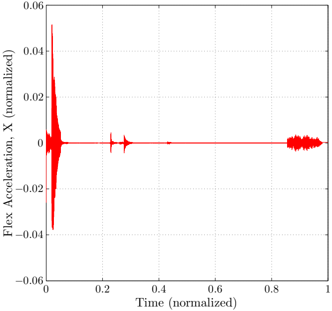

Figure 9: LSQI-DSM

Verification of Energy Conservation

- **Verification of LSQI-DSM approach was performed by examining elastic motion around FEM model transitions**
- **Test case:**
  - Sinusoidal force tuned to the first three bending mode frequencies
  - Force applied via an input grid on the vehicle and intended to provide sufficient excitation over multiple FEM model transitions
  - Goal of test case was to evaluate LSQI-DSM performance without controller interaction
- **The test case provides a comparison of pure DSM, LSQI-DSM, and free decay of the system**
- **Free-decay case used as benchmark to demonstrate elastic behavior in the absence of FEM model transitions**

Verification of Energy Conservation

- **Immediately following FEM model transitions:**
  - Kinetic energy exhibits small amplitude decrease for both methods
  - LSQI-DSM sustains more residual energy across the transition

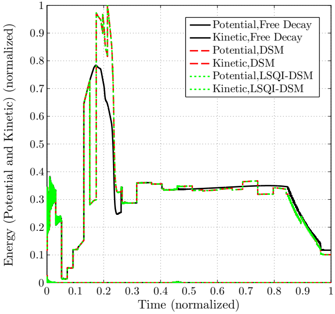

Figure 10: LSQI

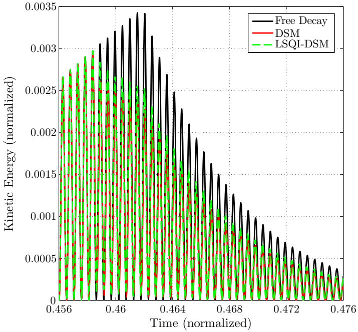

Figure 11: LSQI-DSM

Verification of Energy Conservation

- LSQI-DSM sustains energy across multiple transitions
- Shows a decay rate equivalent to that of the free-decay
- These facts provide validation that LSQI-DSM is not artificially adding or removing energy

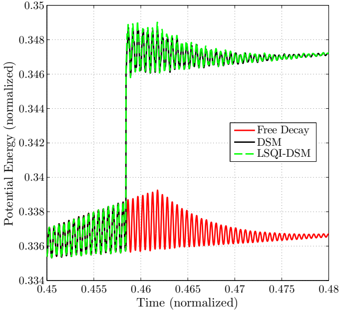

Figure 12: LSQI

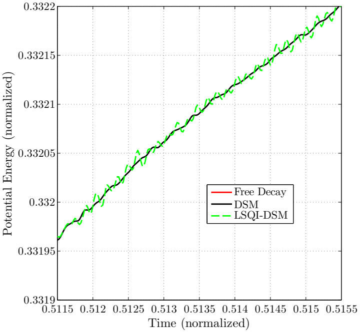

Figure 13: LSQI-DSM

Impact to Vehicle Control Design

- **SLS uses an adaptive controller to modify gains[2]:**
  - Adaptive controller interprets transients as structural instability
  - LSQI-DSM reduces/completely removes the artificial transients, effectively reducing the controller response to the excitation

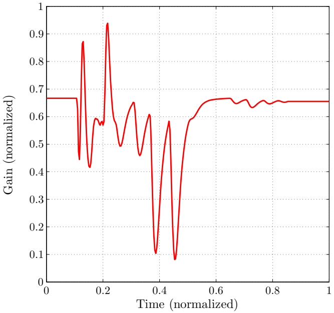

Figure 14: LSQI

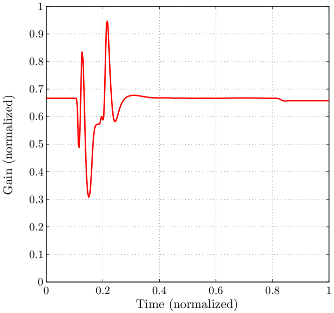

Figure 15: LSQI-DSM

Drawbacks to LSQI-DSM

- **Compared to previous LSQI implementation, LSQI-DSM produces discontinuity in the physical displacements immediately following a transition:**
    1. Results in discontinuous kinematic solution
    2. In presence of inertial navigation, this discontinuity can lead to large inertial navigation errors

- **To solve this problem, consideration in the simulation must be given to ensure kinematic continuity across transitions**

Conclusion

- **The LSQI-DSM method offers appreciable improvement over prior methods by:**
  - Accommodating large changes in system energy between FEM models perpetuated by the use of a truncated mode set
  - Independently addressing the unforced and forced components of the displacement
- **LSQI-DSM shows significant reduction or complete removal of non-physical transients following FEM model transitions:**
  - Positive impact to controller response and navigation solution
  - Sustains elastic motion across multiple FEM model transitions

Space Launch System

Acknowledgments

- The authors would like to thank Jeb Orr of Draper Laboratory for his insight, knowledge, and substantial contributions to the development of LSQI-DSM
- Research and development of the LSQI-DSM method was performed under contract NNM12AA41C

Backup

- **The following slides are backup**

References

- J. Orr, “Elastic Model Transitions Using Quadratic Inequality Constrained Least Squares,” *AIAA Atmospheric Flight Mechanics Conference*, Toronto, CA, 2010.
  AIAA-2010-7642.
- J. Orr and T. VanZwieten, “Robust, Practical Adaptive Control for Launch Vehicles,” August 2012.
  AIAA-2012-15662.
- D. Hodges and G. Pierce, *Introduction to Structural Dynamics and Aeroelasticity*.
  New York, NY: Cambrudge University Press, 2005.
- J. Zapico-Valle, R. Alonso-Camblor, M. González-Martínez, and M. García-Diéguez, “A new method for finite element model updating in structural dynamics,” *Mechanical Systems and Signal Processing*, 2010, pp. 2137–2159.
- J. Mottershead and M. Friswell, “Model Updating in Structural Dynamics: A Survey,” *Journal of Sound and Vibration 167(2)*, 1993, pp. 347–375.
- A. Berman and E. Nagy, “Improvements of a Large Analytical Model Using Test Data,” *Proceedings of the 23rd AIAA/ASME/ASCE/AHS Structures, Structural Dynamics and Materials Conference*, May 1982.
  Paper 82-0743.
- Y. Yang, Y. Chen, and T. Hsu, “Direct Updating Method for Structural Models Based on Orthogonality Constraints,” *Mechanics of Advanced Materials and Structures*, Taylor & Francis, 2009, pp. 390–401.
- B. Jaishi and W. Ren, “Damage detection by finite element model updating using modal flexibility residual,” *Journal of Sound and Vibration 290*, 2006, pp. 347–375.
- A. Kabe, “Mode Shape Identification and Orthogoanlization,” *Proceedings of the 29th AIAA/ASME/ASCE/AHS Structures, Structural Dynamics and Materials Conference*, May 1988.
  Paper 88-2354.